POLITECNICO
MILANO 1863

SCUOLA DI INGEGNERIA INDUSTRIALE
E DELL'INFORMAZIONE

Executive Summary of the Thesis

Quasi-Periodic Orbital Families Performance Analysis for Exoplanets Observation by means of Telescope-Occulter Formation Flying

Laurea Magistrale in Space Engineering - Ingegneria Spaziale

Author: Giorgia Biagetti

Advisor: Prof. Michèle Roberta Lavagna

Co-advisor: Daniele Barberi Spirito

Academic year: 2021-2022

1. Introduction

The study of extra-solar planets represents one of the most ambitious goals to be reached in space science in the near future. Thanks to indirect detection techniques, such as radial velocity-based, transits and gravitational microlensing, the list of known exoplanets has rapidly grown over the years. In particular, in the past few decades, space Telescopes have revolutionized our understanding of Earth-like planets characterizing numerous transiting systems and greatly expanding our knowledge of exoplanets abundance and diversity. However, only direct investigation allows a detailed view of their actual characteristics, like atmospheric composition, physical and orbital properties, and eventually evidence of life. Nevertheless, the enormous contrast between the parent star and the planet imposes strong constraints on this kind of observations, especially in terms of required angular separation. Moreover, despite the success of these missions, they all share one major drawback: they are expensive and complex, especially in terms of technological requirements such as precise calibration of specialized instruments, along with the need for sophisticated data processing and analysis techniques. The inherent complexity of these missions has resulted in a predominant utilization of large-sized satellites. In fact, no exoplanets observation mission has ever flown using CubeSats. Therefore, this study presents a shader concept for exoplanets imaging, based on the Formation Flying (FF) of two small spacecrafts placed on Quasi-Periodic Orbital Families (QPOFs): an Occulter (OSC) designed to provide adequate starlight suppression within its shadow and a conventional Telescope (TSC) to collect the light from the target planet. The main goal of this work is to explore the potential of TSC-OSC orbital and attitude configurations that are more cost-effective and higher-performing for exoplanet observations using the external coronagraph method in a Sun-Earth, non-Keplerian framework. The study intends to provide a general methodology and performance (i.e. Line of Sight achievable pointing accuracy LoS) guidelines to be used for future small-scale Star-shade missions starting from different scientific requirements.

2. Background

The background knowledge needed to approach the present research work is here recalled.

2.1. Dynamical Framework

Despite the reduced number of attractors, the Circular Restricted 3-Body Problem (CR3BP) formulation in Sun-Earth frame represents a valid dynamical model for QPOFs trajectory design. In fact, being the problem autonomous [1], infinite periodic and quasi-periodic solutions may be identified and developed continuously in families. The study focuses the attention on two classes of reference orbits, namely Planar Lyapunov and Halo. Planar Lyapunov Orbits are symmetrical closed trajectories lying in the x-y plane bounded in the proximity of L1 or L2, while Halo Orbits are closed trajectories with both in-plane and out-of-plane components. The most promising alternatives for the studied mission are operative orbits around the L2 Lagrangian point in the Sun-Earth system. These orbits represents a stable environment with a clear view of the sky without interruptions due to Earth occultations. They also provide a wide range of TSC-OSC distances, allowing system design flexibility. Moreover, these orbits are characterized by very small orbital perturbations and absence of relevant radiation sources, thus an appealing condition for a flying cluster operating in formation.

2.2. Periodic Orbits Generation

Periodic orbits repeat over time, so the spacecraft remains in a fixed region of space without the need for constant propulsion. In this work TSC and OSC are placed respectively on a reference periodic and on a toroidal quasi-periodic orbit. The initial guess for the Halo orbits has been generated using the Richardson third-order analytical approximation [2] and a numerical corrector to obtain the periodic solution. Lyapunov instead, are found starting from an initial guess $\mathbf{x_0}$ in the L2 center manifold $\mathbf{x_m(t)}$, propagated forward in time $\mathbf{x(t)}$ using a numerical integrator. Variational equations are then iteratively exploited to identify the direction in which the deviation vector $\mathbf{x(t)} - \mathbf{x_m(t)}$ grows at a constant rate, and used to refine the initial guess for the periodic orbit.

2.3. Quasi-Periodic Orbits Generation

Quasi-Periodic Orbital structures are developed to enable a natural, bounded relative motion between the agents of the Formation, minimizing the control effort and frequency for the maintenance. In this work, a higher order continuation algorithm proposed in [3] for computing QPOFs has been followed. The approach is based on the typical "Prediction-Correction", but it is efficiently designed to speed up the generation of full orbital families, thanks to improved prediction goodness and larger continuation steps.

2.4. Orbit-attitude CR3BP model

In order to propagate orbit-attitude motion simultaneously, Euler equations are included into the classical CR3BP dynamics. Moreover, Solar Radiation Pressure (SRP) is one of the largest perturbations experienced by an object, especially in non-Keplerian trajectories of the Sun-Earth system far from the attractors. For this reason its contribution has been inserted in the rotational dynamics. The system of differential equations [4] can be summarized as:

$$\begin{cases} \dot{\mathbf{x}}_{\mathbf{orb}} = f_{CR3BP}(\mathbf{x_{orb}}) \\ \dot{\mathbf{q}} = f_q(\mathbf{q}, \boldsymbol{\omega}) \\ \dot{\boldsymbol{\omega}} = f_\omega(\mathbf{x_{orb}}, \mathbf{q}, \boldsymbol{\omega}) \end{cases} \tag{1}$$

where $\mathbf{x_{orb}}$ is the state vector of the spacecraft in the CR3BP, $\mathbf{q}$ is the attitude quaternion and $\boldsymbol{\omega}$ is the angular velocity.

3. Mission design

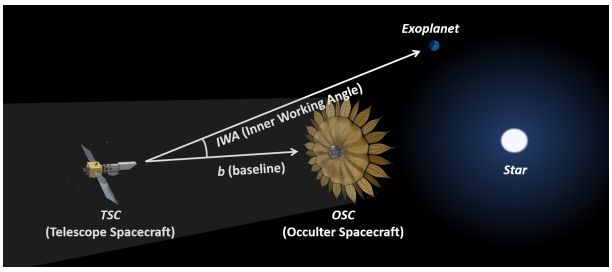

Figure 1: TSC- OSC configuration geometry

3.1. Mission geometry

To maintain the configuration geometry illustrated in Figure 1 and perform the correct FF alignment, high precision is required. The most relevant geometrical parameters involved in the mission design are represented by the baseline b and the Inner Working Angle IWA. In fact, the TSC shall be kept at a range distance b from

the occulting Star-shade, while the TSC is held in the LoS from the Telescope to the target. The TSC instrument pointing error is stringent, but it represents a well-known problem in TSC attitude control so it will not be discussed further in this work. The alignment error θ_{err}, TSC-OSC focal line offset, should be ideally zero. Finally, *IWA* is the other critical quantity for exoplanet observations since it directly affects the acquisitions resolution. It describes the minimum angular distance between the host star and the observed exoplanet that can be resolved by the imaging system.

3.2. Occulter Spacecraft design

The OSC design is analyzed, from both a geometrical and an engineering point of view. Geometric spacecraft design presents the complex relation between all variables involved in the study. For example, a Fresnel number $f > 10$ is preferred because it indicates that the diffraction effects are negligible. Large f values are obtained in the UV spectrum. However, conventional mirror performance sharply degrades for $\lambda < 150\ nm$ and most stars have only a small fraction of their luminous output in this spectrum, meaning longer integration times needed. Again, using greater λ for the science instrument would increase the available flux, but it would decrease the achievable Occulter contrast.
The engineering design discusses the limitations of a circular OSC with respect to a petal-shaped one. In fact the second offers better control over the amount of starlight that leaks around the Occulter edges. The effectiveness of this shape from the optical point of view is related to the number of petals: 12 is the minimum required to be effective, while from 16 onwards it follows an asymptotic trend. The apodization function describes the petal geometry, and some geometric constraints must be satisfied to ensure the OSC is physically realizable. Manufacturing petals and deploying the Star-shade represents one of the major bottlenecks in the OSC design.

3.3. Target selection

Table 1 reports the scientific requirements that must be fulfilled by an exploration mission using an external coronagraph, to effectively detect exoplanets within the habitable zone. By thoroughly analyzing these requirements, we can compile a list of potential targets that are observable with the proposed method.

a [AU]	**d_{Star} [pc]**	**θ_{sep} [arcsec]**	**CR [–]**
0.01-0.1	0.05-50	0.0001-0.1	$\leq 10^{-9}$
D_{tel} [m]	**θ_{res} [arcsec]**	**SNR [–]**	**T_{Obs} [–]**
0.3-10	$\leq \theta_{sep,MAX}$	> 10	$> T_{Orb}$

Table 1: Scientific requirements for exoplanet observation mission using coronagraph method.

4. Performance Analysis

This work aims to investigate the performances of various TSC-OSC orbital configurations for exoplanets observation. To evaluate the system behavior, several metrics such as target area, visibility time, and sky coverage are defined. Additionally, a phase shift is introduced between the reference and toroidal orbit. This section provides a comprehensive comparison between Halo and Lyapunov performances and presents optimal FF configurations. Furthermore, sub-optimal solutions by incorporating attitude dynamics into the problem are explored. The optimization process provides the optimal control torque with SRP contribution. The analysis assesses the acceptable relative pointing precision among the spacecrafts for the proposed approach. The admissible values of pointing errors are then documented with respect to the resultant degradation in the performances, in terms of CR and SNR.

4.1. Orbital optimal analysis

The choice of the observation region for this study was motivated by the high concentration of exoplanets found in the Galactic Center (GC). The desired target area is therefore defined as a cone-shaped region with a 10° aperture, centered in the GC.
The performance parameters to optimize in this study are the sky coverage A_{cov} and visibility time T_{perc}. A_{cov} is computed as the ratio of the total area of the sky covered by the TSC when in visibility of the target to the total area of the observation region, while T_{perc} is the ratio between the time during which the TSC is observing the region of interest to the overall orbital period T_{ref}.
To facilitate the identification of each periodic

and quasi-periodic orbital couple, two simple parameters are introduced: the orbital frequencies Ω_0, related to the periodic motion and Ω_1, which determines the quasi periodic one. Additionally, a shift s between the two spacecrafts is considered, in order to increase the observation region visible with a specific configuration. Doing so, natural motion is exploited without necessarily controlling the orbital dynamics of the TSC-OSC FF, again reducing mission costs. Recalling the shape of the two orbital families, it can be clearly noticed that being the Lyapunov orbits planar, their baseline could ideally cover less region to be observed in the sky. On the contrary, being more inclined trajectories, the elevation vector of the Line of Sight from TSC to OSC for the Halo orbits, spans a broader observation area. Consequently, one would expect performances in terms of Sky Coverage for the Halo case to be higher than Lyapunov ones.
Figures 2 and 3 represent the percentage of area covered by all the different TSC - OSC orbital configurations, defined by the frequency parameters Ω_0 and Ω_1 for each s and validate the predicted results. In fact, maximum performances are obtained for Halo orbital combinations with respect to Lyapunov ones. However, due to the introduction of a phase shift, a wider area of sky observation is achievable also with the Lyapunov family. This justifies the relatively small difference in the A_{cov} peaks for Halo 16.5% compared to 14.3% for the Lyapunov. Similar considerations hold true for the visibility time performance analysis.

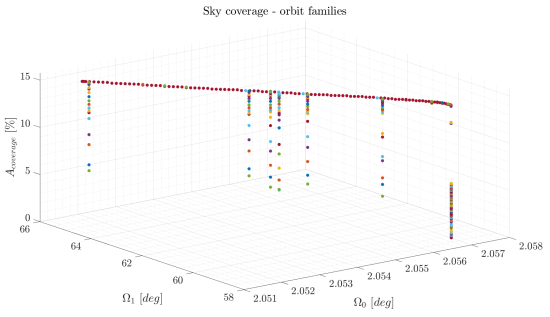

Figure 2: Lyapunov performances: Sky coverage

Once obtained the optimal orbital configurations (reported in Table 4) and the corresponding baseline distances b for each QPOFs, the requirements for attitude analysis need to be

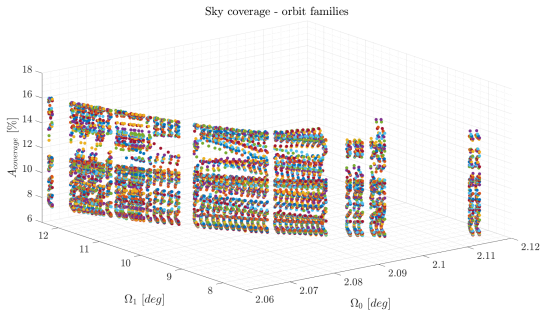

Figure 3: Halo performances: Sky coverage

	Lyapunov	Halo
$\mathbf{\Omega_0}$	2.0513	2.0982
$\mathbf{\Omega_1}$	64.5792	8.2725
$\theta_{\mathbf{shift}}$	30.6°	0.72°

Table 2: Optimal Lyapunov and Halo configurations.

assessed in terms of minimum *IWA* and total pointing error θ_{err}. A maximum lateral offset L_{max} is set to be $< 30\%$ R_{Occ} because beyond this value the optical performances starts to degrade too much, affecting the quality of the observation. So, fixed R_{Occ} and L_{max} values, Table 3 summarizes the attitude performance requirements calculated for both QPOFs. Pointing requirements for Lyapunov orbits are more demanding than Halo ones, since they deal with higher baseline ranges. These parameters will guide the next section calculations.

	b	IWA	θ_{err}
Lyap	$\sim 10^5$ $[km]$	~ 5 $[mas]$	< 0.34 $[mas]$
Halo	$\sim 10^4$ $[km]$	~ 40 $[mas]$	< 2.5 $[mas]$

Table 3: Attitude Performance requirements.

4.2. Attitude sub-optimal analysis

The attitude dynamics performance analysis is conducted starting from the optimal orbits previously found. Sub-optimal control solutions will be therefore explored for different cases. An ideal attitude control optimization is proposed for both Lyapunov and Halo orbits. From now on, all the study will be carried out taking as reference the TSC-OSC Formation from *ECLIPSIS*

mission [5].
In order to find the best control able to maintain the correct FF pointing, the trajectories have been discretized in $n = 1000$ different arcs. The choice of the number n strikes a balance between the accuracy of the state measure and computational cost. For each arc the optimization problem has been defined by imposing the TSC and OSC control torques $M_{c,TSC}$ and $M_{c,OSC}$ as `fsolve` unknown optimization variables x. To create a square problem, the number of variables should be equal to the constraint objective function $F(x)$ dimension, defined as:

$$\mathbf{F(x)} = \begin{cases} \hat{\mathbf{s}}_{\mathbf{B,TSC}} - \hat{\mathbf{x}}_{\mathbf{TSC}} \\ \hat{\mathbf{s}}_{\mathbf{B,OSC}} + \hat{\mathbf{x}}_{\mathbf{OSC}} \end{cases} \tag{2}$$

where $\hat{\mathbf{s}}_{\mathbf{B,TSC}}$ and $\hat{\mathbf{s}}_{\mathbf{B,OSC}}$, are the actual TSC and OSC target pointing vectors expressed in their body frames, calculated from the rotation matrix $\mathbf{R}_{\mathbf{BN_{i-th\ SC}}}$. To cancel the star pointing errors, they should properly be aligned with their $x - axes$ vectors $\hat{x}_{TSC}$ and $\hat{x}_{OSC}$, built so that they coincides with TSC and OSC directions.
For every segment of the trajectory, the optimal outcome from the previous arc is taken as the initial estimate for the successive control torque. The same approach is applied to the initial conditions of the propagator, i.e. $\mathbf{r_0}, \mathbf{v_0}, \mathbf{q_0}, \boldsymbol{\omega_0}$.
To simulate the navigation state reconstruction measurements, an error in the state knowledge is introduced at each step. Measurements are therefore generated by adding random Gaussian noise to the expected state.
To verify the efficiency of the overall FF pointing control, the baseline $\theta_{err,baseline}$ and star misalignment errors $\theta_{err,star}$ are compared and then summed up. Figures 4 and 5 show that $\theta_{err,star}$ results to be smaller than $\theta_{err,baseline}$. This is due to the fact that the attitude control problem has been conducted on accurately selected orbits, in which target visibility was already maximized. Total misalignment error $\theta_{err,total}$ is depicted in red. For Lyapunov configurations attitude requirements are met for the 24.7 % of the orbit, while 28.4 % for Halo. Halo QPOF still allows higher visibility conditions, consistently with previous attitude-free calculations. Moreover, incorporating attitude control to the analysis, those percentages slightly increased, as expected.

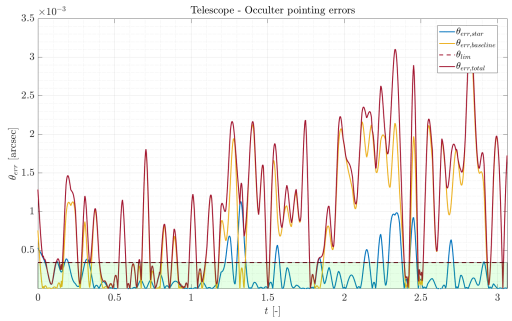

Figure 4: Baseline-Star misalignment errors for Lyapunov orbits

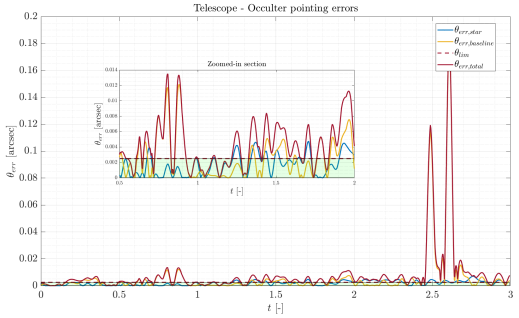

Figure 5: Baseline-Star misalignment errors for Halo orbits

It should be pointed out that exoplanet observations are often done discontinuously, due to the reduced visibility of the target planet. In general, the necessary time to conduct a single scientific imaging can vary from 6 *hours* to 1 *day*. In ECLIPSIS one observation lasts ~ 9.6 *hours*, meaning that for an orbital period of 180 *days*, up to 430 *hours* are completely dedicated to the imaging of a selected target (according to obtained T_{vis}). Moreover, in this work, the occultation method is demonstrated just for a single target, but the study could be greatly expanded if an on-board database was installed on the spacecrafts and a control algorithm was used to align the formation with the direction of the exoplanets present in the FoV at any given time. This would significantly increase the scientific return of the mission. By improving the efficiency of observations, more data could be collected.
However, there are still various trajectories arc in which pointing minimum values are not met. Depending on the mission requirements and ob-

jectives, this may present a significant issue, as any degradation in pointing performance can directly impact the quality of the observation. Therefore, either a reduction in performance should be analyzed, or a better control strategy should be investigated to ensure that the pointing requirements can be met for the entire mission duration.
Figure 6 reveals that when θ_{err} grows, the Signal to Noise Ratio (SNR) decreases because the amount of starlight that reaches the detector increases, making it more difficult to detect the faint light of the exoplanet. The green part of the graph represents the region in which SNR assumes admissible values to perform good exoplanets imaging. The dotted line marks the limit of 10 under which the misalignment error is no more acceptable. Similarly, the impact of $\theta_{err,total}$ on the Contrast Ratio CR can be explained using basic geometric optics.

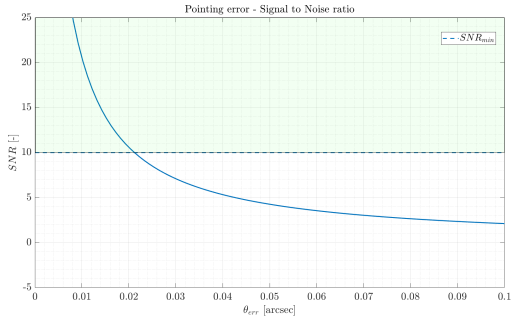

Figure 6: Pointing error - Signal to Noise Ratio

5. Results & Conclusion

The present study encompasses a performance analysis of a TSC-OSC FF mission, implemented for exoplanet observation by utilizing Halo and Lyapunov QPOFs. They are compared in terms of sky coverage and visibility time. The results of the analysis reveal that both families allow exoplanet imaging for about 1/4 of the overall period. Fixed the TSC-OSC geometrical parameters and observed that the baseline distance is in the order of $\sim 10^4 - 10^5$ $[km]$, the constraints on the maximum misalignment error are derived.
At this point, a study on the sub-optimal solutions is performed adding attitude ideal control to the problem to verify if such demanding pointing accuracies could be reached with a feasible M_c applied on the spacecrafts. Calculations show that time in visibility of the target slightly increments for both optimal orbits configurations. To increase scientific return different solutions are viable. Performance degradation with pointing error can be taken into account to understand up to which point good observations can be done. Another option to enhance mission performances could be reducing baseline during scientific imaging or designing a bigger Star-shade. In any case the spacecrafts shall be equipped with very high-performing Attitude Determination and Control System to guarantee *arcsec* pointing accuracy.
Table 4 summarizes the results of the optimal and sub-optimal performance analysis.

	$\mathbf{T_{orb}}$ $[d]$	$\mathbf{b}$ $[km]$	$\mathbf{A_{cov}}$	$\mathbf{T_{vis}}$	$\mathbf{\Delta v}$ $[\frac{m}{s}]$
L	178.15	$\sim 10^5$	14.3%	22.9%	0.507
H	174.16	$\sim 10^4$	16.5%	25.4%	0.610
	$\mathbf{M_c}$ $[Nm]$	$\boldsymbol{\theta_{err}}$ $[as]$	$\mathbf{T_{vis}}$	**SNR**	**CR**
L	10^{-2}	~ 0.1	24.7 %	> 10	$< 10^{-10}$
H	10^{-1}	~ 1	28.4 %	< 10	$> 10^{-10}$

Table 4: Optimal (top) and Sub-optimal (bottom) Performance summary

This work presents a comprehensive study of designing and optimizing a Telescope-Occulter Formation for exoplanets observation. The feasibility of using QPOFs non-Keplerian dynamics for stable Formation has been demonstrated, and the methodology can be adapted to various scenarios. The proposed approach holds immense potential for advancing our understanding of Earth-like planets. However, limitations such as OSC design complexities and technological constraints must be addressed. One promising direction is incorporating attitude with orbital analysis from the beginning of the optimization problem to obtain even better solutions. Multiple OSC in Formation with the TSC and developing on-board algorithms to automatically identify and track exoplanets could enhance performances even more. Moreover, adopting more accurate dynamical models and control strategies, and conducting structural analysis on the Occulter could lead to better outcomes and higher reliability.

References

[1] W. S. Koon, M. W. Lo, J. E. Marsden, and S. D. Ross, "Dynamical systems, the three-body problem and space mission design," pp. 1167–1181, World Scientific, 2000.

[2] D. L. Richardson, "Analytic construction of periodic orbits about the collinear points," *Celestial mechanics*, vol. 22, no. 3, pp. 241–253, 1980.

[3] A. Capannolo, "Dynamics, guidance and control of reconfigurable spacecraft formations in multibody environments," 2022.

[4] A. Colagrossi, *Absolute and Relative 6DOF Dynamics, Guidance and Control for Large Space Structures in Cislunar Environment.* PhD thesis, Politecnico di Milano, 2018.

[5] C. S. e. a. Chillemi E., Colombi F., "Exozodiacal dust imaging for near stars," tech. rep., Politecnico di Milano, 7 2017.

[6] N. J. Kasdin and V. et al., "Recent progress on external occulter technology for imaging exosolar planets," in *2013 IEEE Aerospace Conference*, pp. 1–14, IEEE, 2013.